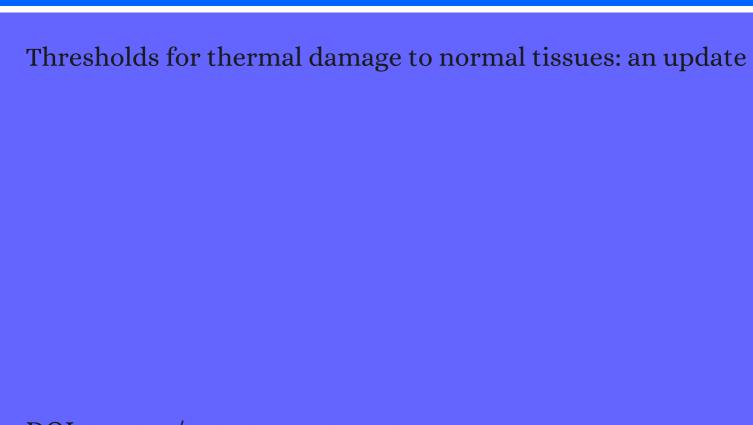
CITATION REPORT List of articles citing



DOI: 10.3109/02656736.2010.534527 International Journal of Hyperthermia, 2011, 27, 320-43.

Source: https://exaly.com/paper-pdf/49858066/citation-report.pdf

Version: 2024-04-28

This report has been generated based on the citations recorded by exaly.com for the above article. For the latest version of this publication list, visit the link given above.

The third column is the impact factor (IF) of the journal, and the fourth column is the number of citations of the article.

#	Paper	IF	Citations
487	Children and adults exposed to electromagnetic fields at the ICNIRP reference levels: theoretical assessment of the induced peak temperature increase. 2011 , 56, 4967-89		43
486	Quality assurance for clinical studies in regional deep hyperthermia. 2011 , 187, 605-10		75
485	Science to practice: Which approaches to combination interventional oncologic therapy hold the greatest promise of obtaining maximal clinical benefit?. 2011 , 261, 667-9		4
484	Children and adults exposed to low-frequency magnetic fields at the ICNIRP reference levels: theoretical assessment of the induced electric fields. 2012 , 57, 1815-29		45
483	Considerations for theoretical modelling of thermal ablation with catheter-based ultrasonic sources: implications for treatment planning, monitoring and control. <i>International Journal of Hyperthermia</i> , 2012 , 28, 69-86	3.7	55
482	Some aspects of quality management in deep regional hyperthermia. <i>International Journal of Hyperthermia</i> , 2012 , 28, 562-9	3.7	21
481	Luciferase-based protein denaturation assay for quantification of radiofrequency field-induced targeted hyperthermia: developing an intracellular thermometer. <i>International Journal of Hyperthermia</i> , 2012 , 28, 202-9	3.7	21
480	Ultrasound increases nanoparticle delivery by reducing intratumoral pressure and increasing transport in epithelial and epithelial-mesenchymal transition tumors. 2012 , 72, 1485-93		73
479	HIFU treatment time reduction through heating approach optimisation. <i>International Journal of Hyperthermia</i> , 2012 , 28, 799-820	3.7	12
478	Concentration and volume effects in thermochemical ablation in vivo: results in a porcine model. <i>International Journal of Hyperthermia</i> , 2012 , 28, 113-21	3.7	13
477	Heat-related injury in lambs. 2012 , 24, 772-6		5
476	Brain temperature: what do we know?. 2012 , 23, 483-7		23
475	MRI-Guided Thermal Ablation Techniques. 2012 , 253-269		
474	Guideline for the clinical application, documentation and analysis of clinical studies for regional deep hyperthermia: quality management in regional deep hyperthermia. 2012 , 188 Suppl 2, 198-211		68
473	Enhanced drug delivery in rabbit VX2 tumours using thermosensitive liposomes and MRI-controlled focused ultrasound hyperthermia. <i>International Journal of Hyperthermia</i> , 2012 , 28, 776-87	3.7	58
472	Mild hyperthermia with magnetic resonance-guided high-intensity focused ultrasound for applications in drug delivery. <i>International Journal of Hyperthermia</i> , 2012 , 28, 320-36	3.7	98
471	Tumour hyperthermia and ablation in rats using a clinical MR-HIFU system equipped with a dedicated small animal set-up. <i>International Journal of Hyperthermia</i> , 2012 , 28, 141-55	3.7	60

470	Ultrasound-mediated micellar drug delivery. International Journal of Hyperthermia, 2012, 28, 374-85	3.7	53
469	Arrhenius analysis of the relationship between hyperthermia and Hsp70 promoter activation: a comparison between ex vivo and in vivo data. <i>International Journal of Hyperthermia</i> , 2012 , 28, 441-50	3.7	11
468	Magnetic resonance-guided high-intensity focused ultrasound (MR-HIFU) ablation of liver tumours. 2012 , 12, 387-94		51
467	Hyperthermia-triggered drug delivery from temperature-sensitive liposomes using MRI-guided high intensity focused ultrasound. 2012 , 161, 317-27		265
466	Dual-wavelength photoacoustic technique for monitoring tissue status during thermal treatments. 2013 , 18, 067003		8
465	CEM43°C thermal dose thresholds: a potential guide for magnetic resonance radiofrequency exposure levels?. 2013 , 23, 2215-27		147
464	Thermal comfort and safety of cotton blankets warmed at 130°F and 200°F. 2013 , 28, 337-46		6
463	Arrhenius parameter determination as a function of heating method and cellular microenvironment based on spatial cell viability analysis. <i>International Journal of Hyperthermia</i> , 2013 , 29, 281-95	3.7	3
462	Low dose of continuous-wave microwave irradiation did not cause temperature increase in muscles tissue adjacent to titanium alloy implantsan animal study. 2013 , 14, 364		6
461	Complete regression of local cancer using temperature-sensitive liposomes combined with ultrasound-mediated hyperthermia. 2013 , 172, 266-273		69
460	An approach to rapid calculation of temperature change in tissue using spatial filters to approximate effects of thermal conduction. 2013 , 60, 1735-41		30
459	Progress and promises of human cardiac magnetic resonance at ultrahigh fields: a physics perspective. 2013 , 229, 208-22		55
458	Radiotherapy in conjunction with superficial and intracavitary hyperthermia for the treatment of solid tumors: survival and thermal parameters. 2013 , 15, 95-105		19
457	Modulation of hyperthermia-induced platelet aggregation inhibition in the presence of urea. <i>International Journal of Hyperthermia</i> , 2013 , 29, 256-8	3.7	2
456	Characterization of Lesion Formation and Bubble Activities during High Intensity Focused Ultrasound Ablation using Temperature-Derived Parameters. 2013 , 60, 108-117		7
455	Comparative analysis of mathematical models of cell death and thermal damage processes. <i>International Journal of Hyperthermia</i> , 2013 , 29, 262-80	3.7	92
454	Cryptorchidism is not a risk factor for antisperm antibody production in post-orchidopexy males with infertility. 2013 , 90, 470-4		8
453	Common gene expression patterns responsive to mild temperature hyperthermia in normal human fibroblastic cells. <i>International Journal of Hyperthermia</i> , 2013 , 29, 38-50	3.7	8

452	Generalised polynomial chaos-based uncertainty quantification for planning MRgLITT procedures. <i>International Journal of Hyperthermia</i> , 2013 , 29, 324-35	3.7	15
451	On the feasibility of concurrent human TMS-EEG-fMRI measurements. 2013 , 109, 1214-27		24
450	Effect of warm compress application on tissue temperature in healthy dogs. 2013, 74, 448-51		8
449	Evolution of the ablation region after magnetic resonance-guided high-intensity focused ultrasound ablation in a Vx2 tumor model. 2013 , 48, 381-6		25
448	Effects of low-dose microwave on healing of fractures with titanium alloy internal fixation: an experimental study in a rabbit model. 2013 , 8, e75756		11
447	Effects of the thermal environment on articular chondrocyte metabolism: a fundamental study to facilitate establishment of an effective thermotherapy for osteoarthritis. 2014 , 17, 14-21		10
446	A clinical trial of neoadjuvant hyperthermic intravesical chemotherapy (HIVEC) for treating intermediate and high-risk non-muscle invasive bladder cancer. <i>International Journal of Hyperthermia</i> , 2014 , 30, 166-70	3.7	29
445	Variable stiffness fabrics with embedded shape memory materials for wearable applications. 2014,		44
444	Optimum temperature for extracellular matrix production by articular chondrocytes. <i>International Journal of Hyperthermia</i> , 2014 , 30, 96-101	3.7	9
443	Photothermal Therapy Using Gold Nanorods and Near-Infrared Light in a Murine Melanoma Model Increases Survival and Decreases Tumor Volume. 2014 , 2014, 1-8		23
442	Conformable actuation and sensing with robotic fabric. 2014 ,		18
441	Science to practice: why debate the role of Dbait for improving tumor ablation?. 2014 , 270, 635-7		
440	Simulation study of the effects of near- and far-field heating during focused ultrasound uterine fibroid ablation using an electronically focused phased array: A theoretical analysis of patient safety. 2014 , 41, 072902		17
439	Evaluation of epidural and peripheral nerve catheter heating during magnetic resonance imaging. 2014 , 39, 534-9		8
438	Vitamin E status and reproduction in sheep: potential implications for Australian sheep production. 2014 , 54, 694		10
437	Thermal tissue damage model analyzed for different whole-body SAR and scan durations for standard MR body coils. <i>Magnetic Resonance in Medicine</i> , 2014 , 71, 421-31	4.4	61
436	Rationalization of thermal injury quantification methods: application to skin burns. 2014 , 40, 896-902		44
435	Polyacrylamide phantom for self-actuating needle-tissue interaction studies. 2014 , 36, 140-5		29

(2015-2014)

434	Experimental characterisation of the thermal lesion induced by microwave ablation. <i>International Journal of Hyperthermia</i> , 2014 , 30, 110-8	47
433	Measurement of SAR-induced temperature increase in a phantom and in vivo with comparison to numerical simulation. <i>Magnetic Resonance in Medicine</i> , 2014 , 71, 1923-31	44
432	Hyperthermia Therapy for Cancer. 2014 , 115-151	4
431	Contact burn due to a heated-wire breathing circuit. 2014 , 28, 802	1
430	Thermoelectrical modeling of bipolar coagulation on posterior spinal artery in a porcine spinal surgery model. 2014 , 61, 182-8	4
429	Implantable magnetic nanocomposites for the localized treatment of breast cancer. 2014 , 116, 233505	16
428	Multiparametric MRI analysis for the evaluation of MR-guided high intensity focused ultrasound tumor treatment. 2015 , 28, 1125-40	9
427	Effects of hyperthermia on DNA repair pathways: one treatment to inhibit them all. 2015 , 10, 165	159
426	Rapid method for thermal dose-based safety supervision during MR scans. 2015 , 36, 398-407	16
425	On the RF heating of coronary stents at 7.0 Tesla MRI. <i>Magnetic Resonance in Medicine</i> , 2015 , 74, 999-101,04	38
424	Compensating for magnetic field inhomogeneity in multigradient-echo-based MR thermometry. **Magnetic Resonance in Medicine*, 2015 , 73, 1184-9 4-4	6
423	The Application of Carbon Nanotubes in Magnetic Fluid Hyperthermia. 2015 , 2015, 1-8	9
422	Biomarkers of multiorgan injury in a preclinical model of exertional heat stroke. 2015 , 118, 1207-20	29
421	Heating and Safety Concerns of the Radio-Frequency Field in MRI. 2015, 3, 1	18
420	Mathematical modeling of the heat-shock response in HeLa cells. 2015, 109, 182-93	23
419	Wireless implantable chip with integrated nitinol-based pump for radio-controlled local drug delivery. 2015 , 15, 1050-8	43
418	Preclinical evaluation of implantable cardioverter-defibrillator developed for magnetic resonance imaging use. 2015 , 12, 631-638	12
417	Safe for Generations to Come. 2015 , 16, 65-84	117

416	Experimental investigation and histopathological identification of acute thermal damage in skeletal porcine muscle in relation to whole-body SAR, maximum temperature, and CEM43 °C due to RF irradiation in an MR body coil of birdcage type at 123 MHz. <i>International Journal of</i>	3.7	14
415	Hyperthermia, 2015, 31, 409-20 Non-lethal heat treatment of cells results in reduction of tumor initiation and metastatic potential. 2015, 464, 51-6		4
414	Novel magnetic heating probe for multimodal cancer treatment. 2015 , 42, 2203-11		6
413	Mechanical and hyperthermic properties of magnetic nanocomposites for biomedical applications. 2015 , 49, 118-28		7
412	Monitoring local heating around an interventional MRI antenna with RF radiometry. 2015 , 42, 1411-23		5
411	Intra-abdominal temperature distribution during consolidation hyperthermic intraperitoneal chemotherapy with carboplatin in the treatment of advanced stage ovarian carcinoma. <i>International Journal of Hyperthermia</i> , 2015 , 31, 396-402	3.7	13
410	Towards a dosimetric framework for therapeutic ultrasound. <i>International Journal of Hyperthermia</i> , 2015 , 31, 182-92	3.7	23
409	Evolution of Thermal Dosimetry for Application of Hyperthermia to Treat Cancer. 2015 , 47, 397-421		23
408	Implantable polymer/metal thin film structures for the localized treatment of cancer by Joule heating. 2015 , 117, 165301		2
407	Trimodal Therapy: Combining Hyperthermia with Repurposed Bexarotene and Ultrasound for Treating Liver Cancer. 2015 , 9, 10695-10718		50
406	Thermal Therapy Approaches for Treatment of Brain Tumors in Animals and Humans. 2016 , 44, 443-457	,	15
405	Investigation of Particle Accumulation, Chemosensitivity and Thermosensitivity for Effective Solid Tumor Therapy Using Thermosensitive Liposomes and Hyperthermia. <i>Theranostics</i> , 2016 , 6, 1717-31	12.1	29
404	Predicting long-term temperature increase for time-dependent SAR levels with a single short-term temperature response. <i>Magnetic Resonance in Medicine</i> , 2016 , 75, 2195-203	4.4	8
403	Electrocautery effect on intestinal vascularisation in a murine model. <i>International Journal of Hyperthermia</i> , 2016 , 32, 643-7	3.7	
402	Near-Infrared-Light-Assisted Photothermal Polymerization for Transdermal Hydrogelation and Cell Delivery. 2016 , 5, 1638-45		18
401	Virtual population-based assessment of the impact of 3 Tesla radiofrequency shimming and thermoregulation on safety and B1 + uniformity. <i>Magnetic Resonance in Medicine</i> , 2016 , 76, 986-97	4.4	32
400	Hyperthermia of magnetic nanoparticles allows passage of sodium fluorescein and Evans blue dye across the blood-retinal barrier. <i>International Journal of Hyperthermia</i> , 2016 , 32, 657-65	3.7	11
399	Normothermic Mouse Functional MRI of Acute Focal Thermostimulation for Probing Nociception. 2016 , 6, 17230		11

(2016-2016)

398	High intensity focused ultrasound induced in vivo large volume hyperthermia under 3D MRI temperature control. 2016 , 43, 1539-49		40
397	Radiofrequency Ablation, MR Thermometry, and High-Spatial-Resolution MR Parametric Imaging with a Single, Minimally Invasive Device. 2016 , 281, 927-932		13
396	Thermal dosimetry for bladder hyperthermia treatment. An overview. <i>International Journal of Hyperthermia</i> , 2016 , 32, 417-33	3.7	24
395	Thermal therapy of pancreatic tumours using endoluminal ultrasound: Parametric and patient-specific modelling. <i>International Journal of Hyperthermia</i> , 2016 , 32, 97-111	3.7	15
394	Sintering of calcium phosphates with a femtosecond pulsed laser for hard tissue engineering. 2016 , 101, 346-354		22
393	Safe use of subdermal needles for intraoperative monitoring with MRI. 2016 , 40, E19		6
392	Ex Vivo HIFU Experiments Using a \$32 times 32\$ -Element CMUT Array. 2016 , 63, 2150-2158		13
391	MRI methods for the evaluation of high intensity focused ultrasound tumor treatment: Current status and future needs. <i>Magnetic Resonance in Medicine</i> , 2016 , 75, 302-17	4.4	35
390	Low-Pressure Burst-Mode Focused Ultrasound Wave Reconstruction and Mapping for Blood-Brain Barrier Opening: A Preclinical Examination. 2016 , 6, 27939		6
389	Hyperthermia. 2016 , 381-398.e6		5
389	Hyperthermia. 2016, 381-398.e6 Effect of thermal dose on heat shock protein expression after radio-frequency ablation with and without adjuvant nanoparticle chemotherapies. <i>International Journal of Hyperthermia</i> , 2016, 32, 829-847	₁ 3·7	5
	Effect of thermal dose on heat shock protein expression after radio-frequency ablation with and	1 ^{3.7}	
388	Effect of thermal dose on heat shock protein expression after radio-frequency ablation with and without adjuvant nanoparticle chemotherapies. <i>International Journal of Hyperthermia</i> , 2016 , 32, 829-84. Comprehensive method to predict and quantify scald burns from beverage spills. <i>International</i>		4
388 387	Effect of thermal dose on heat shock protein expression after radio-frequency ablation with and without adjuvant nanoparticle chemotherapies. <i>International Journal of Hyperthermia</i> , 2016 , 32, 829-84. Comprehensive method to predict and quantify scald burns from beverage spills. <i>International Journal of Hyperthermia</i> , 2016 , 32, 900-910 Endovascular Electrodes for Electrical Stimulation of Blood Vessels for Vasoconstriction - a Finite		4 24
388 387 386	Effect of thermal dose on heat shock protein expression after radio-frequency ablation with and without adjuvant nanoparticle chemotherapies. <i>International Journal of Hyperthermia</i> , 2016 , 32, 829-847. Comprehensive method to predict and quantify scald burns from beverage spills. <i>International Journal of Hyperthermia</i> , 2016 , 32, 900-910. Endovascular Electrodes for Electrical Stimulation of Blood Vessels for Vasoconstriction - a Finite Element Simulation Study. 2016 , 6, 31507		24
388 387 386 385	Effect of thermal dose on heat shock protein expression after radio-frequency ablation with and without adjuvant nanoparticle chemotherapies. <i>International Journal of Hyperthermia</i> , 2016 , 32, 829-84. Comprehensive method to predict and quantify scald burns from beverage spills. <i>International Journal of Hyperthermia</i> , 2016 , 32, 900-910 Endovascular Electrodes for Electrical Stimulation of Blood Vessels for Vasoconstriction - a Finite Element Simulation Study. 2016 , 6, 31507 Reducing temperature elevation of robotic bone drilling. 2016 , 38, 1495-1504		4 24 2 29
388 387 386 385 384	Effect of thermal dose on heat shock protein expression after radio-frequency ablation with and without adjuvant nanoparticle chemotherapies. <i>International Journal of Hyperthermia</i> , 2016 , 32, 829-847. Comprehensive method to predict and quantify scald burns from beverage spills. <i>International Journal of Hyperthermia</i> , 2016 , 32, 900-910 Endovascular Electrodes for Electrical Stimulation of Blood Vessels for Vasoconstriction - a Finite Element Simulation Study. 2016 , 6, 31507 Reducing temperature elevation of robotic bone drilling. 2016 , 38, 1495-1504 A Protocol of Manual Tests to Measure Sensation and Pain in Humans. 2016 , Heat transfer due to electroconvulsive therapy: Influence of anisotropic thermal and electrical skull		4 24 2 29 7

380	Real-time tracking of delayed-onset cellular apoptosis induced by intracellular magnetic hyperthermia. 2016 , 11, 121-36		69
379	Intracranial MR-guided laser-induced thermal therapy: single-center experience with the Visualase thermal therapy system. 2016 , 125, 853-860		79
378	An Overview of Occupational Risks From Climate Change. 2016 , 3, 13-22		28
377	Design of a Subtarsal Ultrasonic Transducer for Mild Hyperthermia Treatment of Dry Eye Disease. 2016 , 42, 232-42		2
376	Method of hyperthermia and tumor size influence effectiveness of doxorubicin release from thermosensitive liposomes in experimental tumors. 2016 , 222, 47-55		45
375	Thermoradiotherapy planning: Integration in routine clinical practice. <i>International Journal of Hyperthermia</i> , 2016 , 32, 41-9	7	44
374	RF safety assessment of a bilateral four-channel transmit/receive 7 Tesla breast coil: SAR versus tissue temperature limits. 2017 , 44, 143-157		6
373	Quality assurance guidelines for superficial hyperthermia clinical trials: I. Clinical requirements. International Journal of Hyperthermia, 2017 , 33, 471-482	7	59
372	A thermoresponsive electromechanical microchip for temperature control in biomedical smart implants. 2017 ,		2
371	On the potential for RF heating in MRI to affect metabolic rates and FDG signal in PET/MR: simulations of long-duration, maximum normal mode heating. 2017 , 44, 589-596		1
370	Thermal Effects of Microwave and Radiofrequency Radiation. 2017, 163-185		
369	Limiting heat loss during surgery in small animals. 2017 , 180, 495-497		1
368	A review of the evidence for threshold of burn injury. 2017 , 43, 1624-1639		33
367	Pre-operative Screening and Manual Drilling Strategies to Reduce the Risk of Thermal Injury During Minimally Invasive Cochlear Implantation Surgery. 2017 , 45, 2184-2195		4
366	Mild external heating and reduction in spontaneous contractions of the bladder. 2017 , 120, 724-730		1
365	Modeling and Experimental Analysis of Thermal Therapy during Short Pulse Laser Irradiation. 2017 , 243-25	9	
364	Thermal Skin Damage During Reirradiation and Hyperthermia Is Time-Temperature Dependent. 2017 , 98, 392-399		19
363	Facile construction of mitochondria-targeting nanoparticles for enhanced phototherapeutic effects. 2017 , 5, 1022-1031		18

(2017-2017)

362	The incidence of nerve root injury by high-speed drill can be reduced by chilled saline irrigation in a rabbit model. 2017 , 99-B, 554-560	8
361	Croconaine nanoparticles with enhanced tumor accumulation for multimodality cancer theranostics. 2017 , 129, 28-36	50
360	. 2017 , 65, 1795-1806	50
359	Integrated HIFU Drive System on a Chip for CMUT-Based Catheter Ablation System. 2017 , 11, 534-546	14
358	Microwave ablation of renal tumors: A narrative review of technical considerations and clinical results. 2017 , 98, 287-297	30
357	Equivalence of cell survival data for radiation dose and thermal dose in ablative treatments: analysis applied to essential tremor thalamotomy by focused ultrasound and gamma knife. 3.7 International Journal of Hyperthermia, 2017, 33, 401-410	8
356	Synergistic effects of heat and antibiotics on Pseudomonas aeruginosa biofilms. 2017, 33, 855-866	18
355	Regulating Near-Infrared Photodynamic Properties of Semiconducting Polymer Nanotheranostics for Optimized Cancer Therapy. 2017 , 11, 8998-9009	199
354	Increasing Distribution of Drugs Released from In Situ Forming PLGA Implants Using Therapeutic Ultrasound. 2017 , 45, 2879-2887	9
353	Effect of Frequency and Focal Spacing on Transcranial Histotripsy Clot Liquefaction, Using Electronic Focal Steering. 2017 , 43, 2302-2317	15
352	Review of the progress toward achieving heat confinement-the holy grail of photothermal therapy. 2017 , 22, 80901	34
351	Transcutaneous Recharge: A Comparison of Numerical Simulation to In Vivo Experiments. 2017 , 20, 613-621	5
350	Cranial arterial patterns of the alpaca (Camelidae:). 2017 , 4, 160967	6
349	Blood and Heat Transfer. 2017 , 227-264	O
348	Real-time temperature monitoring and estimation of thermal damage in pancreas undergoing magnetic resonance-guided laser ablation: First in vivo study. 2017 ,	1
347	Efficacy of monopolar dielectric transmission radio frequency in panniculus adiposus and cellulite reduction. 2017 , 19, 422-426	4
346	3D radiobiological evaluation of combined radiotherapy and hyperthermia treatments. **International Journal of Hyperthermia*, 2017, 33, 160-169** 3-7	22
345	Nd3+ activated CaF2 NPs as colloidal nanothermometers in the biological window. 2017 , 68, 29-34	35

344	Preclinical MRI-Guided Focused Ultrasound: A Review of Systems and Current Practices. 2017, 64, 291-3	305	12
343	Three-Dimensional Microwave Hyperthermia for Breast Cancer Treatment in a Realistic Environment Using Particle Swarm Optimization. 2017 , 64, 1335-1344		30
342	Survey on Preclinical Methods to Assess Collateral Thermal Damage to Tissues Caused by Surgical Devices. 2017 , 19, 63-73		
341	Safety of Simultaneous Scalp or Intracranial EEG during MRI: A Review. 2017 , 5,		11
340	pH- and temperature-responsive nanosystems. 2017 , 281-315		
339	Albumin-Gold Nanorod Nanoplatform for Cell-Mediated Tumoritropic Delivery with Homogenous ChemoDrug Distribution and Enhanced Retention Ability. <i>Theranostics</i> , 2017 , 7, 3034-3052	12.1	19
338	Flexible Medical Devices: Review of Controllable Stiffness Solutions. 2017 , 6, 23		95
337	Tumor Stiffening, a Key Determinant of Tumor Progression, is Reversed by Nanomaterial-Induced Photothermal Therapy. <i>Theranostics</i> , 2017 , 7, 329-343	12.1	45
336	New experimental model for single liver lobe hyperthermia in small animals using non-directional microwaves. 2017 , 12, e0184810		2
335	Effects of Low Intensity Continuous Ultrasound (LICU) on Mouse Pancreatic Tumor Explants. 2017 , 7, 1275		2
334	Mitochondrial fission contributes to heat-induced oxidative stress in skeletal muscle but not hyperthermia in mice. 2018 , 200, 6-14		16
333	Thermal shock susceptibility and regrowth of Pseudomonas aeruginosa biofilms. <i>International Journal of Hyperthermia</i> , 2018 , 34, 168-176	3.7	11
332	Photothermal Therapy Generates a Thermal Window of Immunogenic Cell Death in Neuroblastoma. 2018 , 14, e1800678		104
331	Analysis of clinical data to determine the minimum number of sensors required for adequate skin temperature monitoring of superficial hyperthermia treatments. <i>International Journal of Hyperthermia</i> , 2018 , 34, 910-917	3.7	12
330	Is Edema a Matter of Concern After Laser Ablation of Epileptogenic Focus?. 2018, 113, 366-372.e3		5
329	Motion Correction in Proton Resonance Frequency-based Thermometry in the Liver. 2018 , 27, 53-61		9
328	Mechanical fractionation of tissues using microsecond-long HIFU pulses on a clinical MR-HIFU system. <i>International Journal of Hyperthermia</i> , 2018 , 34, 1213-1224	3.7	10
327	Principles of focused ultrasound. 2018 , 27, 41-50		13

326	Safety Aspects of Non-Thermal Plasmas. 2018 , 83-109	5
325	Three-Dimensional Printing of Cytocompatible, Thermally Conductive Hexagonal Boron Nitride Nanocomposites. 2018 , 18, 3488-3493	67
324	Establishment of a human intrapleural hyperthermic perfusion model and analysis of pleural malignancy treatment depth. 2018 , 138, 144-149	2
323	Transurethral high-intensity ultrasound for treatment of stress urinary incontinence (SUI): simulation studies with patient-specific models. <i>International Journal of Hyperthermia</i> , 2018 , 34, 1236-1247	4
322	Magnetic Particle Imaging-Guided Heating in Vivo Using Gradient Fields for Arbitrary Localization of Magnetic Hyperthermia Therapy. 2018 , 12, 3699-3713	204
321	Effect of applied voltage, duration and repetition frequency of RF pulses for pain relief on temperature spikes and electrical field: a computer modelling study. <i>International Journal of 3.7 Hyperthermia</i> , 2018 , 34, 112-121	15
320	Measurement and analysis of the impact of time-interval, temperature and radiation dose on tumour cell survival and its application in thermoradiotherapy plan evaluation. <i>International Journal of Hyperthermia</i> , 2018 , 34, 30-38	21
319	SAR Simulations & Safety. 2018 , 168, 33-58	46
318	Technical aspects of osteoid osteoma ablation in children using MR-guided high intensity focussed ultrasound. <i>International Journal of Hyperthermia</i> , 2018 , 34, 49-58	18
317	An In Vitro and Numerical Study of Moxibustion Therapy on Biological Tissue. 2018 , 65, 779-788	8
316	Micromixing using swirling induced by three-dimensional dual surface acoustic waves (3D-dSAW). 2018 , 255, 3434-3440	25
315	Self-Assembly of Thermoresponsive Recombinant Silk-Elastinlike Nanogels. 2018 , 18, 1700192	11
314	Estimates for the acoustical stimulation and heating of multiphase biotissue. 2018 , 17, 717-725	1
313	Potential for thermal damage to the blood-brain barrier during craniotomy: implications for intracortical recording microelectrodes. 2018 , 15, 034001	18
312	Oxygenic Hybrid Semiconducting Nanoparticles for Enhanced Photodynamic Therapy. 2018 , 18, 586-594	234
311	A stepping micromotor based on ferrofluid bearing for side-viewing microendoscope applications. 2018 , 269, 258-268	11
310	Investigation of Thermal Distribution of Balloon Antenna MWA for Urethra Stricture Treatment. 2018 ,	
309	Low-Temperature Burn on Replanted Fingers and Free Flaps in Hand. 2018 , 81, 402-406	1

308	HIFU Drive System Miniaturization Using Harmonic Reduced Pulsewidth Modulation. 2018, 65, 2407-2417	5
307	CIROFOMITE (Crystallization Inhibitor of Uric Acid in Synovial Fluid with Implanted Thermoregulator). 2018 ,	
306	A micro-pipette thermal sensing technique for measuring the thermal conductivity of non-volatile fluids. 2018 , 89, 114902	1
305	Magnetic Relaxation of Agglomerated and Immobilized Iron Oxide Nanoparticles for Hyperthermia and Imaging Applications. 2018 , 9, 1-5	10
304	Thermogenetic stimulation of single neocortical pyramidal neurons transfected with TRPV1-L channels. 2018 , 687, 153-157	5
303	Planar coil-based contact-mode magnetic stimulation: synaptic responses in hippocampal slices and thermal considerations. 2018 , 8, 13423	2
302	Voltaglue Bioadhesives Energized with Interdigitated 3D-Graphene Electrodes. 2018 , 7, e1800538	21
301	Comparison of effectiveness of epidural analgesia and monitored anesthesia care for high-intensity focused ultrasound treatment of adenomyosis. <i>International Journal of Hyperthermia</i> , 2018 , 35, 617-625 $^{3.7}$	1
300	Feasibility of targeting canine soft tissue sarcoma with MR-guided high-intensity focused ultrasound. <i>International Journal of Hyperthermia</i> , 2019 , 35, 205-215	5
299	Combining Bulk Temperature and Nanoheating Enables Advanced Magnetic Fluid Hyperthermia Efficacy on Pancreatic Tumor Cells. 2018 , 8, 13210	37
298	Self-Healing and Adhesive Artificial Tissue Implant for Voice Recovery 2018, 1, 1134-1146	16
297	Precisely Striking Tumors without Adjacent Normal Tissue Damage via Mitochondria-Templated Accumulation. 2018 , 12, 6252-6262	49
296	Biophysical and photobiological basics of water-filtered infrared-A hyperthermia of superficial tumors. <i>International Journal of Hyperthermia</i> , 2018 , 35, 26-36	21
295	Manipulating the mitochondria activity in human hepatic cell line Huh7 by low-power laser irradiation. 2018 , 9, 1283-1300	17
294	Magnetic Hyperthermia and Radiation Therapy: Radiobiological Principles and Current Practice. 2018 , 8,	81
293	Higher environmental temperatures promote acceleration of spermatogenesis in vivo in mice (Mus musculus). 2018 , 77, 14-23	9
292	Magnetic (Hyper)Thermia or Photothermia? Progressive Comparison of Iron Oxide and Gold Nanoparticles Heating in Water, in Cells, and In Vivo. 2018 , 28, 1803660	114
291	Transurethral Microwave Thermotherapy for Treatment of Benign Prostatic Hyperplasia. 2018 , 131-141	

29 0	Cellular Obstruction Clearance in Proximal Ventricular Catheters Using Low-Voltage Joule Heating. 2018 , 65, 2503-2511	1
289	Establishing sheep as an experimental species to validate ultrasound-mediated blood-brain barrier opening for potential therapeutic interventions. <i>Theranostics</i> , 2018 , 8, 2583-2602	21
288	Predicting lesion size by accumulated thermal dose in MR-guided focused ultrasound for essential tremor. 2018 , 45, 4704-4710	31
287	Influence of hyperthermal regimes on experimental teratoma development in vitro. 2018 , 99, 131-144	4
286	Managing Heat Stress Episodes in Confined Cattle. 2018 , 34, 325-339	11
285	Changes in the specific absorption rate (SAR) of radiofrequency energy in patients with retained cardiac leads during MRI at 1.5T and 3T. <i>Magnetic Resonance in Medicine</i> , 2019 , 81, 653-669 4.4	20
284	Three-dimensional biomimetic head model as a platform for thermal testing of protective goggles for prevention of eye injuries. 2019 , 64, 35-41	7
283	Immersed in Thermal Flows: Heat as Productive of and Produced by Social Practices. 2019 , 129-148	5
282	Thermotolerance of camel (Camelus dromedarius) somatic cells affected by the cell type and the dissociation method. 2019 , 26, 29490-29496	5
281	Safety and penetration of light into the brain. 2019 , 49-66	2
280	Thermal Effects Associated with RF Exposures in Diagnostic MRI: Overview of Existing and Emerging Concepts of Protection. 2019 , 2019, 1-17	9
279	Emission Spectroscopic Characterization of a Helium Atmospheric Pressure Plasma Jet with Various Mixtures of Argon Gas in the Presence and the Absence of De-Ionized Water as a Target. 2019 , 2, 283-293	5
278	A multi-segmented shape memory alloy-based actuator system for endoscopic applications. 2019 , 296, 92-100	16
277	Evaluating HIFU-mediated local drug release using thermal strain imaging: Phantom and preliminary in-vivo studies. 2019 , 46, 3864-3876	7
276	Development of temperature controller-integrated portable HIFU driver for thermal coagulation. 2019 , 18, 77	2
275	A new experimental model of muscle pain in humans based on short-wave diathermy. 2019 , 23, 1733-1742	2
274	Battery-free, fully implantable optofluidic cuff system for wireless optogenetic and pharmacological neuromodulation of peripheral nerves. 2019 , 5, eaaw5296	79
273	Numerical simulation of magnetic fluid hyperthermia based on multiphysics coupling and recommendation on preferable treatment conditions. 2019 , 19, 1031-1039	10

272	Temperature and thermal dose during radiotherapy and hyperthermia for recurrent breast cancer are related to clinical outcome and thermal toxicity: a systematic review. <i>International Journal of Hyperthermia</i> , 2019 , 36, 1024-1039	7	39
271	Predicting high-intensity focused ultrasound thalamotomy lesions using 2D magnetic resonance thermometry and 3D Gaussian modeling. 2019 , 46, 5722-5732		6
270	Comparison of block and pulsed radiofrequency of the ganglion impar in coccygodynia. 2019 , 49, 1555-155	59	8
269	A Photo-Stable Indocyanine Green and Rapamycin Co-Delivery System Based on Poly(Glutamic Acid)-Modified Manganese Phosphate for Synergetic Tumor Therapy. 2019 , 5, 1477-1487		1
268	Temperature control in TTFields therapy of GBM: impact on the duty cycle and tissue temperature. 2019 , 64, 225008		8
267	Finite Element Method Guided Measurement of Temperature Profile in Tissue Exposed to a Transcutaneous Energy Transfer System. 2019 ,		
266	Using the body to self-cool a 10 W transcutaneous energy transfer system. 2019 ,		
265	Flexible and Lightweight Devices for Wireless Multi-Color Optogenetic Experiments Controllable via Commercial Cell Phones. 2019 , 13, 819		13
264	Role of Simulations in the Treatment Planning of Radiofrequency Hyperthermia Therapy in Clinics. 2019 , 2019, 9685476		10
263	Histopathological evaluation of prostate specimens after thermal ablation may be confounded by the presence of thermally-fixed cells. <i>International Journal of Hyperthermia</i> , 2019 , 36, 915-925	7	O
262	Efficient shear wave elastography using transient acoustic radiation force excitations and MR displacement encoding. <i>Magnetic Resonance in Medicine</i> , 2019 , 81, 3153-3167	4	2
261	Liver Tumor Spheroid Reconstitution for Testing Mitochondrial Targeted Magnetic Hyperthermia Treatment. 2019 , 5, 1635-1644		8
260	Melationship between thermal dose and cell death for "rapid" ablative and "slow" hyperthermic heating Winternational Journal of Hyperthermia, 2019, 36, 229-243	7	15
259	Targeted laser therapy synergistically enhances efficacy of antibiotics against multi-drug resistant Staphylococcus aureus and Pseudomonas aeruginosa biofilms. 2019 , 20, 102018		20
258	Externally Addressable Smart Drug Delivery Vehicles: Current Technologies and Future Directions. 2019 , 31, 4971-4989		41
257	Magnetic hyperthermia adjunctive therapy for fungi: studies against. <i>International Journal of Hyperthermia</i> , 2019 , 36, 545-553	7	4
256	Deployable cylindrical phased-array applicator mimicking a concentric-ring configuration for minimally-invasive delivery of therapeutic ultrasound. 2019 , 64, 125001		4
255	Radiofrequency-Sensitive Longitudinal Relaxation Tuning Strategy Enabling the Visualization of Radiofrequency Ablation Intensified by Magnetic Composite. 2019 , 11, 11251-11261		19

254	NIR light-responsive short peptide/2D NbSe2 nanosheets composite hydrogel with controlled-release capacity. 2019 , 7, 3134-3142	15
253	A Thermal Aware Routing Algorithm for a Wireless Body Area Network. 2019 , 105, 1353-1380	17
252	Concurrent Thermochemoradiotherapy in Glioblastoma Treatment: Preliminary Results. 2019,	
251	Human Cardiac Magnetic Resonance at Ultrahigh Fields. 2019 , 142-160.e4	
250	Endobronchial high-intensity ultrasound for thermal therapy of pulmonary malignancies: simulations with patient-specific lung models. <i>International Journal of Hyperthermia</i> , 2019 , 36, 1108-112 3^{-7}	6
249	Feasibility and safety assessment of magnetic resonance-guided high-intensity focused ultrasound (MRgHIFU)-mediated mild hyperthermia in pelvic targets evaluated using an porcine model. 3.7 International Journal of Hyperthermia, 2019, 36, 1147-1159	8
248	Optimization of the order and spacing of sequences in an MRI exam to reduce the maximum temperature and thermal dose. <i>Magnetic Resonance in Medicine</i> , 2019 , 81, 2161-2166	2
247	The utility of bone scintigraphy with SPECT/CT in the evaluation and management of frostbite injuries. 2019 , 92, 20180545	6
246	Near-infrared light control of bone regeneration with biodegradable photothermal osteoimplant. 2019 , 193, 1-11	97
245	3D Manipulation of an Active Steerable Needle via Actuation of Multiple SMA Wires. 2020 , 38, 410-426	6
244	Light-induced modulation of the mitochondrial respiratory chain activity: possibilities and limitations. 2020 , 77, 2815-2838	17
243	Assembling a thermal rhythmanalysis: Energetic flows, heat stress and polyrhythmic interactions in the context of climate change. 2020 , 108, 275-285	10
242	Identifying the Role of Block Length in Neural Heat Block to Reduce Temperatures During Infrared Neural Inhibition. 2020 , 52, 259-275	5
241	Defining Thermally Safe Laser Lithotripsy Power and Irrigation Parameters: Model. <i>Journal of Endourology</i> , 2020 , 34, 76-81	13
241		13
	Endourology, 2020 , 34, 76-81	
240	Endourology, 2020, 34, 76-81 Association of Liver Tissue Optical Properties and Thermal Damage. 2020, 52, 779-787	16

236	Urodynamic assessment of bladder storage function after radical hysterectomy for cervical cancer. 2020 , 133, 2274-2280	1
235	Cold Atmospheric Plasma Treatment for Pancreatic Cancer-The Importance of Pancreatic Stellate Cells. <i>Cancers</i> , 2020 , 12,	5
234	Characterization of magnetic resonance-guided high-intensity focused ultrasound (MRgHIFU)-induced large-volume hyperthermia in deep and superficial targets in a porcine model. International Journal of Hyperthermia, 2020, 37, 1159-1173	2
233	Thermal dose as a universal tool to evaluate nanoparticle-induced photothermal therapy. 2020 , 587, 119657	6
232	Hyperthermia can alter tumor physiology and improve chemo- and radio-therapy efficacy. 2020 , 163-164, 98-124	32
231	Closed-Loop Temperature Control Based on Fiber Bragg Grating Sensors for Laser Ablation of Hepatic Tissue. 2020 , 20,	14
230	Thermogenetics as a New Direction in Controlling the Activity of Neural Networks. 2020 , 50, 1018-1023	3
229	Engineering Materials at the Nanoscale for Triboelectric Nanogenerators. 2020 , 1, 100142	59
228	Temperature effect on the PpIX production during the use of topical precursors. 2020 , 30, 101786	O
227	Numerical modelling of temperature increase induced by transcutaneous Spinal Direct Current Stimulation (tsDC). 2020 ,	
226	. 2020 , 3, 466-469	3
225	A simulated model for fluid and tissue heating during pediatric laser lithotripsy. 2020 , 16, 626.e1-626.e8	3
224	Thermochromic Tissue Phantoms for Evaluating Temperature Distribution in Simulated Clinical Applications of Pulsed Electric Field Therapies. 2020 , 2, 362-371	
223	Microglia Activation and Inflammation During the Death of Mammalian Photoreceptors. 2020 , 6, 149-169	7
222	wIRA-heating of piglet skin and subcutis: proof of accordance with ESHO criteria for superficial hyperthermia. <i>International Journal of Hyperthermia</i> , 2020 , 37, 887-896	2
221	An Insight to the Role of Thermal Effects on the Onset of Atrioesophageal Fistula: A Computer Model of Open-Irrigated Radiofrequency Ablation. 2020 , 11, 481-493	2
220	Design of Silicon Photonic Structures for Multi-Site, Multi-Spectral Optogenetics in the Deep Brain. 2020 , 12, 1-7	1
219	Evaluation of human brain hyperthermia using exergy balance equation. 2020 , 93, 102723	

(2020-2020)

218	An incoherent HIFU transducer for treatment of the medial branch nerve: Numerical study and in vivo validation. <i>International Journal of Hyperthermia</i> , 2020 , 37, 1219-1228	3.7	2
217	An overview of mathematical models and modulated-heating protocols for thermal ablation. 2020 , 52, 489-541		3
216	Electro-thermal therapy: Microsecond duration pulsed electric field tissue ablation with dynamic temperature control algorithms. 2020 , 121, 103807		4
215	Bilayer Hydrogel Sheet-Type Intraocular Microrobot for Drug Delivery and Magnetic Nanoparticles Retrieval. 2020 , 9, e2000118		21
214	Mathematical modeling of the thermal effects of irreversible electroporation for , , and clinical use: a systematic review. <i>International Journal of Hyperthermia</i> , 2020 , 37, 486-505	3.7	20
213	Mammalian cell sensitivity to hyperthermia in various cell lines: a new universal and predictive description. <i>International Journal of Hyperthermia</i> , 2020 , 37, 506-516	3.7	6
212	Acoustic streaming effect on flow and heat transfer in porous tissue during exposure to focused ultrasound. 2020 , 21, 100670		9
211	Cancer cells resist hyperthermia due to its obstructed activation of caspase 3. 2020 , 25, 323-326		4
210	Poly(dl-Lactic Acid)-Based Linear Polyurethanes Capable of Forming Physical Crosslinking via UPy Quadruple Hydrogen Bonding Assembly. 2020 , 305, 2000042		2
209	Continuous, noninvasive wireless monitoring of flow of cerebrospinal fluid through shunts in patients with hydrocephalus. 2020 , 3, 29		14
209		18	14 5
	patients with hydrocephalus. 2020 , 3, 29	18	
208	Optical Focusing beyond the Diffraction Limit via Vortex-Assisted Transient Microlenses. 2020 , 7, 914-9	18	5
208	patients with hydrocephalus. 2020, 3, 29 Optical Focusing beyond the Diffraction Limit via Vortex-Assisted Transient Microlenses. 2020, 7, 914-9 Amplitude Modulation Method for Acoustic Radiation Force Impulse Excitation. 2020, 69, 2429-2438 Thermal distribution, physiological effects and toxicities of extracorporeally induced whole-body	18	5
208	Optical Focusing beyond the Diffraction Limit via Vortex-Assisted Transient Microlenses. 2020, 7, 914-9. Amplitude Modulation Method for Acoustic Radiation Force Impulse Excitation. 2020, 69, 2429-2438 Thermal distribution, physiological effects and toxicities of extracorporeally induced whole-body hyperthermia in a pig model. 2020, 8, e14366 Ultrasound-Enhanced Chemiluminescence for Bioimaging. 2020, 8, 25 Feasibility study of MR-guided pancreas ablation using high-intensity focused ultrasound in a	18 3·7	5 1 2
208 207 206 205	Optical Focusing beyond the Diffraction Limit via Vortex-Assisted Transient Microlenses. 2020, 7, 914-9. Amplitude Modulation Method for Acoustic Radiation Force Impulse Excitation. 2020, 69, 2429-2438 Thermal distribution, physiological effects and toxicities of extracorporeally induced whole-body hyperthermia in a pig model. 2020, 8, e14366 Ultrasound-Enhanced Chemiluminescence for Bioimaging. 2020, 8, 25 Feasibility study of MR-guided pancreas ablation using high-intensity focused ultrasound in a		5 1 2 7
208 207 206 205 204	Optical Focusing beyond the Diffraction Limit via Vortex-Assisted Transient Microlenses. 2020, 7, 914-9 Amplitude Modulation Method for Acoustic Radiation Force Impulse Excitation. 2020, 69, 2429-2438 Thermal distribution, physiological effects and toxicities of extracorporeally induced whole-body hyperthermia in a pig model. 2020, 8, e14366 Ultrasound-Enhanced Chemiluminescence for Bioimaging. 2020, 8, 25 Feasibility study of MR-guided pancreas ablation using high-intensity focused ultrasound in a healthy swine model. <i>International Journal of Hyperthermia</i> , 2020, 37, 786-798 Spatial mapping of tissue properties in vivo reveals a 3D stiffness gradient in the mouse limb bud.		5 1 2 7 3

200	Moderate hyperthermic heating encountered during thermal ablation increases tumor cell activity. <i>International Journal of Hyperthermia</i> , 2020 , 37, 119-129	3.7	13
199	Mild magnetic nanoparticle hyperthermia enhances the susceptibility of biofilm to antibiotics. <i>International Journal of Hyperthermia</i> , 2020 , 37, 66-75	3.7	21
198	Heat transfer analysis in an uncoiled model of the cochlea during magnetic cochlear implant surgery. 2020 , 154, 119683-119683		2
197	Therapeutic ultrasound experiments in vitro: Review of factors influencing outcomes and reproducibility. 2020 , 107, 106167		15
196	A Soft, Biocompatible Magnetic Field Enabled Wireless Surgical Lighting Patty for Neurosurgery. 2020 , 10, 2001		4
195	Green Light-Based Photobiomodulation with an Implantable and Biodegradable Fiber for Bone Regeneration. 2020 , 4, 1900879		7
194	Dual-sectored transurethral ultrasound for thermal treatment of stress urinary incontinence: in silico studies in 3D anatomical models. 2020 , 58, 1325-1340		О
193	Guidelines for Limiting Exposure to Electromagnetic Fields (100 kHz to 300 GHz). <i>Health Physics</i> , 2020 , 118, 483-524	2.3	389
192	MRI-Related Heating of Implants and Devices: A Review. 2021 , 53, 1646-1665		26
191	Modelling of the Temperature Changes Induced by Transcutaneous Spinal Direct Current Stimulation (tsDCS). 2021 , 5, 9-16		О
190	Stray energy transfer in single-incision robotic surgery. <i>Surgical Endoscopy and Other Interventional Techniques</i> , 2021 , 35, 2981-2985	5.2	О
189	Brain and Human Body Modeling 2020. 2021 ,		2
188	Multi-Tissue Analysis on the Impact of Electroporation on Electrical and Thermal Properties. 2021 , 68, 771-782		6
187	Design of Hyperthermia Applicator to Heat Multi-Brain Tumors Simultaneously Based on Adaptive Beamforming Technique. 2021 , 5, 115-123		1
186	Magnetic Resonance Guided Navigation of Untethered Microgrippers. 2021 , 10, e2000869		6
185	Temperature profiles of calyceal irrigation fluids during flexible ureteroscopic Ho:YAG laser lithotripsy. 2021 , 53, 415-419		3
184	A computational investigation of strain concentration in the brain in response to a rapid temperature rise. 2021 , 115, 104228		4
183	Effect of Chilled Irrigation on Caliceal Fluid Temperature and Time to Thermal Injury Threshold During Laser Lithotripsy: Model. <i>Journal of Endourology</i> , 2021 , 35, 700-705	2.7	6

182	Inorganic Nanomaterials for Photothermal-Based Cancer Theranostics. 2021, 4, 2000207		5
181	Quantitative prediction of the extent of pelvic tumour ablation by magnetic resonance-guided high intensity focused ultrasound. <i>International Journal of Hyperthermia</i> , 2021 , 38, 1111-1125	3.7	
180	Hyperspectral Imagery for Assessing Laser-Induced Thermal State Change in Liver. 2021, 21,		6
179	Effect of gastrointestinal gas on the temperature distribution in pancreatic cancer hyperthermia treatment planning. <i>International Journal of Hyperthermia</i> , 2021 , 38, 229-240	3.7	O
178	Exploring the rationale for thermotherapy in COVID-19. <i>International Journal of Hyperthermia</i> , 2021 , 38, 202-212	3.7	3
177	activity of hyperthermia on swarming motility and antimicrobial susceptibility profiles of isolates. <i>International Journal of Hyperthermia</i> , 2021 , 38, 1002-1012	3.7	3
176	Closed-loop trans-skull ultrasound hyperthermia leads to improved drug delivery from thermosensitive drugs and promotes changes in vascular transport dynamics in brain tumors. <i>Theranostics</i> , 2021 , 11, 7276-7293	12.1	7
175	Safety evaluation of long-term temperature controlled whole-body thermal treatment in female Aachen minipig. <i>International Journal of Hyperthermia</i> , 2021 , 38, 165-175	3.7	2
174	A review of intervention methods used to reduce flying-fox mortalities in heat stress events. 2021 , 43, 137		2
173	Sensing non-light-absorbing media via thermally modulated photoacoustic measurements. 2021 , 118, 023701		1
172	Implications of mmWave Radiation on Human Health: State of the Art Threshold Levels. 2021 , 9, 13009)-1302 <i>°</i>	1 2
171	Deep-tissue localization of magnetic field hyperthermia using pulse sequencing. <i>International Journal of Hyperthermia</i> , 2021 , 38, 743-754	3.7	2
170	Non-Thermal, Selective Cancer Treatment With High-Frequency Medium-Intensity Focused Ultrasound 2021 , 9, 122051-122066		О
169	Review on the advancements of magnetic gels: towards multifunctional magnetic liposome-hydrogel composites for biomedical applications. 2021 , 288, 102351		9
168	Iterative time-reversal for multi-frequency hyperthermia. 2021, 66, 045027		10
167	Radiofrequency Electromagnetic Fields. 1-32		
166	Wireless and battery-free technologies for neuroengineering. 2021,		26
165	Thermal exposure of implant osteotomies and its impact on osseointegration-A preclinical in vivo study. 2021 , 32, 672-683		O

164	Combining target coverage and hot-spot suppression into one cost function: the hot-to-cold spot quotient. 2021 ,	3
163	Soft, Wireless and subdermally implantable recording and neuromodulation tools. 2021,	4
162	Modulating the Heat Stress Response to Improve Hyperthermia-Based Anticancer Treatments. <i>Cancers</i> , 2021 , 13,	7
161	Group Refractive Index of Nanocrystalline Yttria-Stabilized Zirconia Transparent Cranial Implants. 2021 , 9, 619686	
160	Continuous versus Intermittent Application of Electric Fields during TTFields for Glioblastoma Treatment. 2021 ,	
159	Sub-minute prediction of brain temperature based on sleep-wake state in the mouse. 2021 , 10,	4
158	The Role of Skeletal Muscles in Exertional Heat Stroke Pathophysiology. 2021 , 42, 673-681	2
157	Towards a Wristed Percutaneous Robot With Variable Stiffness for Pericardiocentesis. 2021 , 6, 2993-3000	1
156	Finite element simulation and integration of CEM43 °C and Arrhenius Models for ultrasonic-assisted skull bone grinding: A thermal dose model. 2021 , 90, 9-22	5
155	Focused ultrasound radiosensitizes human cancer cells by enhancement of DNA damage. 2021 , 197, 730-743	4
154	Predicting final lesion characteristics during MR-guided focused ultrasound pallidotomy for treatment of ParkinsonMdisease. 2020 , 134, 1083-1090	7
153	Simultaneous CMOS-Based Imaging of Calcium Signaling of the Central Amygdala and the Dorsal Raphe Nucleus During Nociception in Freely Moving Mice. 2021 , 15, 667708	2
152	Low-intensity ultrasound restores long-term potentiation and memory in senescent mice through pleiotropic mechanisms including NMDAR signaling. 2021 ,	5
151	The Effects of Localized Heat on the Hallmarks of Cancer. 2021 , 4, 2000267	3
150	An implantable optogenetic stimulator wirelessly powered by flexible photovoltaics with near-infrared (NIR) light. 2021 , 180, 113139	6
149	Transcervical microwave ablation in type 2 uterine fibroids via a hysteroscopic approach: analysis of ablation profiles. 2021 , 7,	O
148	In situ printing of scaffolds for reconstruction of bone defects. 2021 , 127, 313-326	12
147	Radiobiological Evaluation of Combined Gamma Knife Radiosurgery and Hyperthermia for Pediatric Neuro-Oncology. <i>Cancers</i> , 2021 , 13,	1

146	Temperature Assessment of a Novel Pulsed Thulium Solid-State Laser Compared with a Holmium:Yttrium-Aluminum-Garnet Laser. <i>Journal of Endourology</i> , 2021 , 35, 853-859	2.7	1
145	Feedback-controlled thermal therapy of tissues based on fiber Bragg grating thermometers. 2021 ,		
144	A Side-Viewing Endoscopic Probe With Distal Micro Rotary Scanner for Multimodal Luminal Imaging and Analysis. 2021 , 30, 433-441		0
143	AAPM Task Group 241: A medical physicist guide to MRI-guided focused ultrasound body systems. 2021 , 48, e772-e806		2
142	Transferred Cold Atmospheric Plasma Treatment on Melanoma Skin Cancer Cells with/without Catalase Enzyme In Vitro. 2021 , 11, 6181		O
141	Pelvicaliceal Volume and Fluid Temperature Elevation During Laser Lithotripsy. <i>Journal of Endourology</i> , 2021 ,	2.7	4
140	Using focal cooling to link neural dynamics and behavior. 2021 , 109, 2508-2518		2
139	Inhibition of swarming motility using in vitro hyperthermia. 2021 , 100, 102955		1
138	Rapid safety assessment and mitigation of radiofrequency induced implant heating using small root mean square sensors and the sensor matrix Q. <i>Magnetic Resonance in Medicine</i> , 2022 , 87, 509-527	4.4	1
137	External Basic Hyperthermia Devices for Preclinical Studies in Small Animals. <i>Cancers</i> , 2021 , 13,	6.6	6
136	Suitability of eigenvalue beam-forming for discrete multi-frequency hyperthermia treatment planning. 2021 , 48, 7410-7426		2
135	Theoretical Evaluation of Microwave Ablation Applied on Muscle, Fat and Bone: A Numerical Study. 2021 , 11, 8271		1
134	Environment Responsive Metal-Organic Frameworks as Drug Delivery System for Tumor Therapy. 2021 , 16, 140		2
133	Experimental Validation of a Three-Dimensional Heat Transfer Model Within the Scala Tympani With Application to Magnetic Cochlear Implant Surgery. 2021 , 68, 2821-2832		1
132	Chilled irrigation for control of temperature elevation during ureteroscopic laser lithotripsy: in vivo porcine model. <i>Journal of Endourology</i> , 2021 ,	2.7	1
131	Biaxial mechanics of thermally denaturing skin - Part 1: Experiments. 2021 , 140, 412-412		O
130	Variable Molecular Weight Polymer Nanoparticles for Detection and Hyperthermia-Induced Chemotherapy of Colorectal Cancer. <i>Cancers</i> , 2021 , 13,	6.6	1
129	Genetically Encoded Protein Thermometer Enables Precise Electrothermal Control of Transgene Expression. 2021 , 8, e2101813		4

128	A three-dimensional thermal model of the human cochlea for magnetic cochlear implant surgery. 2021 , 178, 121553		О
127	. 2021 , 56, 2913-2923		1
126	A combined modelling and experimental study of heat shock factor SUMOylation in response to heat shock. 2021 , 530, 110877		
125	Treatment planning facilitates clinical decision making for hyperthermia treatments. <i>International Journal of Hyperthermia</i> , 2021 , 38, 532-551	3.7	5
124	PID Controlling Approach Based on FBG Array Measurements for Laser Ablation of Pancreatic Tissues. 2021 , 70, 1-9		2
123	In silico assessment of collateral eddy current heating in biocompatible implants subjected to magnetic hyperthermia treatments. <i>International Journal of Hyperthermia</i> , 2021 , 38, 846-861	3.7	3
122	Photothermal therapies to improve immune checkpoint blockade for cancer. <i>International Journal of Hyperthermia</i> , 2020 , 37, 34-49	3.7	11
121	magnetic nanoparticle hyperthermia: a review on preclinical studies, low-field nano-heaters, noninvasive thermometry and computer simulations for treatment planning. <i>International Journal of Hyperthermia</i> , 2020 , 37, 76-99	3.7	23
120	Three-dimensional tissue stiffness mapping in the mouse embryo supports durotaxis during early limb bud morphogenesis.		3
119	Thermographic analysis of photodynamic therapy with intense pulsed light and needle-free injection photosensitizer delivery: an animal study. 2018 ,		1
118	Interstitial magnetic thermotherapy dosimetry based on shear wave magnetomotive optical coherence elastography. 2019 , 10, 539-551		9
117	Tumor selective hyperthermia induced by short-wave capacitively-coupled RF electric-fields. 2013 , 8, e68506		52
116	Multiparametric MRI analysis for the identification of high intensity focused ultrasound-treated tumor tissue. 2014 , 9, e99936		22
115	Avoiding thermal injury during near-infrared photoimmunotherapy (NIR-PIT): the importance of NIR light power density. 2017 , 8, 113194-113201		20
114	Instant Stress: Detection of Perceived Mental Stress Through Smartphone Photoplethysmography and Thermal Imaging. 2019 , 6, e10140		22
113	Therapeutic exercise and radiofrequency in the rehabilitation project for hip osteoarthritis pain. 2020 , 56, 451-458		5
112	Using a Qualitative Phenomenological Approach to Inform the Etiology and Prevention of Occupational Heat-Related Injuries in Australia. 2020 , 17,		5
111	Magnetic Micromanipulation for Measurement of Stiffness Heterogeneity and Anisotropy in the Mouse Mandibular Arch. 2020 , 2020, 7914074		6

110	Modulated-Power Implantable Neuromodulation Devices and Their Impact on Surrounding Tissue Temperatures. 2016 , 09, 545-562	3
109	The Performance of a Novel Latching-Type Electromagnetic Actuator for Single-Port Laparoscopic Surgery. 2019 , 10, 1659-1673	2
108	HSP90 inhibition acts synergistically with heat to induce a pro-immunogenic form of cell death in colon cancer cells. <i>International Journal of Hyperthermia</i> , 2021 , 38, 1443-1456	7 1
107	Assessment of Human Exposure to Electromagnetic Fields: Review and Future Directions. 2021 , 63, 1619-	1630 ₁₇
106	Perches as Cooling Devices for Reducing Heat Stress in Caged Laying Hens: A Review. 2021 , 11,	3
105	Vital signal sensing and manipulation of a microscale organ with a multifunctional soft gripper. 2021 , 6, eabi6774	8
104	Image-Guided Thermal Therapy. 2013 , 689-726	
103	Heating of infusion fluids through heated breathing circuits. 2017 , 12, 28-31	
102	Short Pulse Laser Based Thermal Therapy. 2017 , 23-39	
101	Pre-clinical validation of transrectal diffuse optical tomography for monitoring photocoagulation progression during photothermal therapy of prostate cancer. 2019 ,	
100	A Thermal Study of Tumor-Treating Fields for Glioblastoma Therapy. 2021 , 37-62	2
99	A Sub-Minute Resolution Prediction of Brain Temperature Based on Sleep-Wake State in the Mouse.	1
98	Engineered Red Blood Cell Biomimetic Nanovesicle with Oxygen Self-Supply for Near-Infrared-II Fluorescence-Guided Synergetic Chemo-Photodynamic Therapy against Hypoxic Tumors. 2021 ,	6
97	Assessment of the efficiency of different chemical treatments and ultrasonic cleaning for defatting of cancellous bone samples. 2021 , 1	O
96	Temperature Dynamics in Rat Brains Exposed to Near-Field Waveguide Outputs at 2.8 GHz. 2021,	1
95	A Hydrogel Ionic Circuit Based High-Intensity Iontophoresis Device for Intraocular Macromolecule and Nanoparticle Delivery. 2021 , e2107315	3
94	Toward a Patient-Specific Image Data-Driven Predictive Modeling Framework for Guiding Microwave Ablative Therapy. 2020 , 198-207	
93	Parameterizing the Effects of Tumor Shape in Magnetic Nanoparticle Thermotherapy Through a Computational Approach. 2021 ,	О

92	Optical plasmonic star-shaped nanoprobes for intracellular sensing and imaging. 2021 , 53, 1		0
91	MRI-Guided Therapy. 2020 , 65, 1427-1435		1
90	The development of microfabricated solenoids with magnetic cores for micromagnetic neural stimulation. <i>Microsystems and Nanoengineering</i> , 2021 , 7, 91	7.7	3
89	Dual Photothermal/Chemotherapy of Melanoma Cells with Albumin Nanoparticles Carrying Indocyanine Green and Doxorubicin Leads to Immunogenic Cell Death. 2021 , e2100353		2
88	Flexible optoelectric neural interfaces. 2021 , 72, 121-130		1
87	Functional Monitoring and Imaging in Deep Brain Structures. 2021 , 1-32		
86	Laser-Induced Thermal Treatment of Superficial Human Tumors: An Advanced Heating Strategy and Non-Arrhenius Law for Living Tissues. 2022 , 1,		1
85	Hazard identification for consumer-grade Head-Mounted Displays (HMDs). 2021 ,		
84	Constraint Removal for MPC with Performance Preservation and a Hyperthermia Cancer Treatment Case Study. 2021 ,		0
83	Clinical Evidence for Thermometric Parameters to Guide Hyperthermia Treatment <i>Cancers</i> , 2022 , 14,	6.6	O
82	Trans-Spinal Focused Ultrasound Stimulation Selectively Modulates Descending Motor Pathway <i>IEEE Transactions on Neural Systems and Rehabilitation Engineering</i> , 2022 , PP,	4.8	0
81	Fast Adaptive Temperature-Based Re-Optimization Strategies for On-Line Hot Spot Suppression during Locoregional Hyperthermia <i>Cancers</i> , 2021 , 14,	6.6	1
80	How Safe is Plasma Treatment in Clinical Applications?. 2022 , 99-126		0
79	Theranostic nanoparticles for the management of thrombosis <i>Theranostics</i> , 2022 , 12, 2773-2800	12.1	O
78	Is Tecar Therapy Effective on Biceps Femoris and Quadriceps Rehabilitation? A Cadaveric Study <i>Journal of Sport Rehabilitation</i> , 2022 , 1-8	1.7	0
77	How Does Cold Plasma Work in Medicine?. 2022 , 63-86		O
76	Progress in Understanding Radiofrequency Heating and Burn Injuries for Safer MR Imaging <i>Magnetic Resonance in Medical Sciences</i> , 2022 ,	2.9	0
75	Efficacy of Radiofrequency as Therapy and Diagnostic Support in the Management of Musculoskeletal Pain: A Systematic Review and Meta-Analysis <i>Diagnostics</i> , 2022 , 12,	3.8	Ο

(2019-2022)

74	Laser operator duty cycle effect on temperature and thermal dose: in-vitro study <i>World Journal of Urology</i> , 2022 , 1	4	О
73	Thermal-Corrosion-Free Electrode-Integrated Cell Chip for Promotion of Electrically Stimulated Neurite Outgrowth. <i>Biochip Journal</i> , 2022 , 16, 99-110	4	1
72	Accurate Three-Dimensional Thermal Dosimetry and Assessment of Physiologic Response Are Essential for Optimizing Thermoradiotherapy <i>Cancers</i> , 2022 , 14,	6.6	3
71	Effects of Non-Invasive Radiofrequency Diathermy in Pelvic Floor Disorders: A Systematic Review <i>Medicina (Lithuania)</i> , 2022 , 58,	3.1	O
70	Does the Novel Thulium Fiber Laser Have a Higher Risk of Urothelial Thermal Injury than the Conventional Holmium Laser in an In Vitro Study?. <i>Journal of Endourology</i> , 2022 ,	2.7	O
69	Deep regional hyperthermia combined with modern concurrent chemoradiotherapy increases T-downstaging rate in locally advanced rectal cancer <i>International Journal of Hyperthermia</i> , 2022 , 39, 431-436	3.7	
68	Hardware-Efficient Compression of Neural Multi-Unit Activity Using Machine Learning Selected Static Huffman Encoders.		O
67	Generated temperatures and thermal laser damage during upper tract endourological procedures using the holmium: yttrium-aluminum-garnet (Ho:YAG) laser: a systematic review of experimental studies World Journal of Urology, 2022, 1	4	O
66	High-voltage long-duration pulsed radiofrequency attenuates neuropathic pain in CCI rats by inhibiting Cav2.2 in spinal dorsal horn and dorsal root ganglion <i>Brain Research</i> , 2022 , 1785, 147892	3.7	
65	Safety of MRI in patients with retained cardiac leads <i>Magnetic Resonance in Medicine</i> , 2021 ,	4.4	O
64	A standard test phantom for the performance assessment of magnetic resonance guided high intensity focused ultrasound (MRgHIFU) thermal therapy devices <i>International Journal of Hyperthermia</i> , 2022 , 39, 57-68	3.7	1
63	Non-thermal Electroporation Ablation of Epileptogenic Zones Stops Seizures in Mice While Providing Reduced Vascular Damage and Accelerated Tissue Recovery <i>Frontiers in Behavioral Neuroscience</i> , 2021 , 15, 774999	3.5	O
62	Ultrasounds in cancer therapy: A summary of their use and unexplored potential <i>Oncology Reviews</i> , 2022 , 16, 531	4.3	О
61	Enhanced Therapeutic Effect of Liposomal Doxorubicin Bio-Orthogonal Chemical Reactions in Tumors <i>Molecular Pharmaceutics</i> , 2022 ,	5.6	Ο
60	Ho:YAG laser and temperature: is it safe to use high-power settings?. World Journal of Urology, 2022 , 1	4	О
59	Data_Sheet_1.pdf. 2019 ,		
58	Video_1.MP4. 2019 ,		
57	Video_2.MP4. 2019 ,		

56	Scale Effects on Performance of BLDC Micromotors for Internal Biomedical Applications: a Finite Element Analysis. <i>Journal of Medical Devices, Transactions of the ASME</i> , 2022 ,	1.3	3
55	Cutaneous steam burns and steam inhalation injuries: a literature review and a case presentation. European Journal of Plastic Surgery,	0.6	О
54	Clinical Intervention Using Focused Ultrasound (FUS) Stimulation of the Brain in Diverse Neurological Disorders. <i>Frontiers in Neurology</i> , 2022 , 13,	4.1	1
53	Potential Application of CEM43 °C and Arrhenius Model in Neurosurgical Bone Grinding. <i>Materials Forming, Machining and Tribology</i> , 2022 , 145-158	0.5	О
52	Analysis of ICNIRP 2020 Basic Restrictions for Localized Radiofrequency Exposure in the Frequency Range Above 6 GHz. <i>Health Physics</i> , 21 , Publish Ahead of Print,	2.3	
51	Robotic stray energy with constant-voltage versus constant-power regulating electrosurgical generators. Surgical Endoscopy and Other Interventional Techniques,	5.2	
50	Temperature assessment study of ex vivo holmium laser enucleation of the prostate model. <i>World Journal of Urology</i> ,	4	
49	Tissue engineering approaches for the in vitro production of spermatids to treat male infertility: A review. <i>European Polymer Journal</i> , 2022 , 111318	5.2	О
48	A PEDOT nano-composite for hyperthermia and elimination of urological bacteria. 2022, 212994		О
47	Efficacy and hazards of 425 nm oral cavity light dosing to inactivate SARS-CoV-2. <i>Journal of Dentistry</i> , 2022 , 104203	4.8	
46	IoT based thermal aware routing protocols in wireless body area networks: Survey: IoT based thermal aware routing in WBAN. <i>IET Communications</i> ,	1.3	1
46 45		1.3 7.7	1
	thermal aware routing in WBAN. <i>IET Communications</i> , Enhancing metabolic activity and differentiation potential in adipose mesenchymal stem cells via high-resolution surface-acoustic-wave contactless patterning. <i>Microsystems and Nanoengineering</i> ,		
45	thermal aware routing in WBAN. <i>IET Communications</i> , Enhancing metabolic activity and differentiation potential in adipose mesenchymal stem cells via high-resolution surface-acoustic-wave contactless patterning. <i>Microsystems and Nanoengineering</i> , 2022, 8,		
45	thermal aware routing in WBAN. <i>IET Communications</i> , Enhancing metabolic activity and differentiation potential in adipose mesenchymal stem cells via high-resolution surface-acoustic-wave contactless patterning. <i>Microsystems and Nanoengineering</i> , 2022, 8, Wireless Neuromodulation at Submillimeter Precision via a Microwave Split-Ring Resonator. Characterization of fluid dynamics and temperature profiles during ureteroscopy with laser		1
45 44 43	thermal aware routing in WBAN. <i>IET Communications</i> , Enhancing metabolic activity and differentiation potential in adipose mesenchymal stem cells via high-resolution surface-acoustic-wave contactless patterning. <i>Microsystems and Nanoengineering</i> , 2022, 8, Wireless Neuromodulation at Submillimeter Precision via a Microwave Split-Ring Resonator. Characterization of fluid dynamics and temperature profiles during ureteroscopy with laser activation in a model ureter		
. Anti-Fn14-Conjugated Prussian Blue Nanoparticles as a Targeted Photothermal Therapy Agent for		0	
45 44 43 42	thermal aware routing in WBAN. <i>IET Communications</i> , Enhancing metabolic activity and differentiation potential in adipose mesenchymal stem cells via high-resolution surface-acoustic-wave contactless patterning. <i>Microsystems and Nanoengineering</i> , 2022, 8, Wireless Neuromodulation at Submillimeter Precision via a Microwave Split-Ring Resonator. Characterization of fluid dynamics and temperature profiles during ureteroscopy with laser activation in a model ureter		
. Anti-Fn14-Conjugated Prussian Blue Nanoparticles as a Targeted Photothermal Therapy Agent for Glioblastoma. 2022, 12, 2645 Assessment of intrarenal temperature dynamics when using holmium and thulium: YAG lasers in an | | 0 |

38	A patterns of care analysis of hyperthermia in combination with radio(chemo)therapy or chemotherapy in European clinical centers.	О
37	Chitosan-Based Scaffolds for Facilitated Endogenous Bone Re-Generation. 2022 , 15, 1023	3
36	The Role of Intraperitoneal Intraoperative Chemotherapy with Paclitaxel in the Surgical Treatment of Peritoneal Carcinomatosis from Ovarian Cancer yperthermia versus Normothermia: A Randomized Controlled Trial. 2022 , 11, 5785	0
35	Temperature analysis of 3D-printed biomaterials during unipolar and bipolar radiofrequency ablation procedure. 9,	1
34	Evaluation of Active Warming and Surgical Draping for Perioperative Thermal Support in Laboratory Mice. 2022 , 61, 482-494	0
33	Short-pulsed micro-magnetic stimulation of the vagus nerve. 13,	0
32	Transcranial Non-genetic Neuromodulation Via Bioinspired Vesicle-Enabled Precise NIR-II Optical-stimulation. 2208601	0
31	Estimation of Heat Diffusion in Human Tissue at Adverse Temperatures Using the Cylindrical Form of Bioheat Equation. 2022 , 10, 3820	O
30	Tissue damage-tracking control system for image-guided photothermal therapy of cancer. 2,	O
29	Evaluacifi de la dinfinica de la temperatura intrarrenal con el uso de l\(\mathbb{B}\)eres holmio y tulio YAG en un modelo ex vivo de ri\(\mathbb{B}\) porcino. 2022 ,	O
28	Hardware-Efficient Compression of Neural Multi-Unit Activity. 2022, 10, 117515-117529	0
27	Wireless Fully-passive Neural Recorder with Artifact Reduction by Optical Chopping. 2022,	0
26	Lessons Learned from Two Decades of Modeling the Heat-Shock Response. 2022 , 12, 1645	О
25	A highly Efficacious Electrical Biofilm Treatment System for Combating Chronic Wound Bacterial Infections. 2208069	0
24	Organelle-targeted therapies: a comprehensive review on system design for enabling precision oncology. 2022 , 7,	2
23	Rhythm Mild-temperature Photothermal Therapy Enhancing Immunogenic Cell Death Response in Oral Squamous Cell Carcinoma. 2202360	O
22	The hot-to-cold spot quotient for SAR-based treatment planning in deep microwave hyperthermia. 2022 , 39, 1421-1439	2
21	A study of flex miniaturized coils for focal nerve magnetic stimulation.	o

20	Piezo-Activated Atomic-Thin Molybdenum Disulfide/MXene Nanoenzyme for Integrated and Efficient Tumor Therapy via Ultrasound-Triggered Schottky Electric Field. 2205053	O
19	Assessing critical temperature dose areas in the kidney by magnetic resonance imaging thermometry in an ex vivo Holmium: YAG laser lithotripsy model.	O
18	Sol-gel dip-coated TiO2 nanofilms reduce heat production in titanium alloy implants produced by microwave diathermy. 2023 , 40,	0
17	An endoluminal cylindrical sectored-ring ultrasound phased-array applicator for minimally-invasive therapeutic ultrasound.	O
16	Towards an integrated RF safety concept for implant carriers in MRI based on sensor-equipped implants and parallel transmission.	0
15	The Rise of Heatstroke as a Method of Depopulating Pigs and Poultry: Implications for the US Veterinary Profession. 2023 , 13, 140	O
14	Bibliography. 2018 ,	0
13	Functional Monitoring and Imaging in Deep Brain Structures. 2023 , 3055-3086	O
12	Simultaneous proton resonance frequency T 1 - MR shear wave elastography for MR-guided focused ultrasound multiparametric treatment monitoring.	0
11	Selective Infrared Neural Inhibition Can Be Reproduced by Resistive Heating. 2023,	O
10	Effect of porous heat transfer model on different equivalent thermal dose methods considering an experiment-based nanoparticle distribution during magnetic hyperthermia. 2023 , 56, 145402	0
9	Neural modulation with photothermally active nanomaterials. 2023 , 1, 193-207	1
8	Modeling of Ultrasound Stimulation of Adolescent Pancreas for Insulin Release Therapy.	0
7	Active implantable medical devices Requirements and test protocols for safety of patients with pacemakers and ICDs exposed to magnetic resonance imaging. 2021 ,	O
6	A coupled finite-volume immersed boundary method for the simulation of bioheat transfer in 3D complex tumor.	0
5	A Magnetically Actuated Variable Stiffness Manipulator Based on Deployable Shape Memory Polymer Springs. 2200465	O
4	Patient-specific simulation of high-intensity focused ultrasound for head and neck cancer ablation. 2023 , 37, 2119-2130	O
3	The Effects of Energy on the Relationship between the Acoustic Focal Region and Biological Focal Region during Low-Power Cumulative HIFU Ablation. 2023 , 13, 4492	0

Dual-frequency piezoelectric micromachined ultrasound transducer based on polarization switching in ferroelectric thin film.

О

Photothermal Therapy for Cancer Treatment. 2023, 755-780

C